# Towards optimal experimental conditions in dynamic contrast-enhanced MRI the influence of injection parameters

Aerts, H.J.W.L.

*Award date:*
2006

Eindhoven University of Technology
Department of Biomedical Engineering & Electrical Engineering
BIOMIM & Control Systems

TU/e technische universiteit eindhoven

# Towards optimal experimental conditions in dynamic contrast-enhanced MRI: the influence of injection parameters

by Hugo Aerts

Master of Science thesis

Project period: January 2005– November 2005
Report Number: 05A/08
Commissioned by:
Prof.dr.ir. P.P.J. van den Bosch

Supervisors:
Dr.ir. N.A.W. v. Riel
Dr.ir. A.A.H. Damen
Dr.ir. W.H. Backes UM/AZM

**Abstract**

The development of dynamic contrast-enhanced magnetic resonance imaging (DCE-MRI) is of growing importance for the detection and characterizations of tumors. Pharmacokinetic models and parameter estimation have been introduced to quantify the microvascular properties of the tumor. System and identification theory provides insights on experimental design. Using a frequency analysis and a "Monte Carlo" simulation study, a theoretic investigation of the injection parameters on the predictability and reliability of the pharmacokinetic parameters was performed to find the optimal experimental conditions. A new tracer distribution model (TDM) was developed to describe the relation between the injection and the arterial input function (AIF). Both the injection rate (in ml/s) as the injection volume (in ml) have been shown to be of great importance for reliable results. For optimal results, the injection rate and injection volume should be as high as possible, both for a manual injection or the usage of an automated pump. Small injection volumes (< 15 ml) and small injection rates (< 2 ml/s) should be avoided, otherwise a large inaccuracy must be expected. Multiple injections, when the volume is divided in multiple parts in time, did not improve the reliability and therefore a single injection is favorable.

*Keywords:* *Injection Shape; Tracer Distribution Model (TDM); Optimal Experimental Conditions; Arterial Input Function (AIF); Pharmacokinetic Model; Optimal Excitation;*

## Introduction

The development of dynamic contrast-enhanced magnetic resonance imaging (DCE-MRI) has led to a non-invasive technique for the characterization of tumors. The leakage rate of a low-molecular-weight extracellular contrast agent (such as Gd-DTPA) into the tumor tissue gives insight in physiological properties of the tumor, like the permeability and the relative volume of the interstitial space [1] [2]. DCE-MRI is beginning to play a central role in the evaluation of novel therapies, for example anti-angiogenesis drugs and gene and antibody therapies [1] [2]. For an oncologist it is of growing importance to have a reliable and accurate assessment of the tumor angiogenesis, to get the proper information for a treatment plan and the possibility to monitor the therapy effectively [8][11]. Pharmacokinetic models and parameter estimation have been introduced to describe the concentration-vs.-time curves of the contrast agent to quantify these microvascular properties [3] [4].

A pharmacokinetic model should have enough parameters to approach the complexity of the actual physiology on the one hand, but also a limited number of parameters such that they are identifiable from the measurement data, on the other hand. This trade-off between complexity and identifiability is often referred to as "minimal modeling". A commonly used pharmacokinetic model is a two-compartment model [3][4][6], which uses kinetic parameters to describe the exchange of contrast agent between two compartments: the blood plasma and the extravascular extracellular space (EES). The concentration in the arterial blood plasma is the input and the concentration in the tissue is the output of the model. When these concentration curves are obtained from the DCE-MRI data, the kinetic parameters can be calculated with numerical methods. Current standards in calculating these kinetic parameters in DCE-MRI show great variation in predictability and reliability [7]. The explanation can be sought in the mathematical structure [21] and the experimental conditions, where recent investigations have been focused on sample time, signal-to-noise ratio (SNR) and experiment duration [21][10]. To build forward on this research an investigation about the influence of the injection shape has been performed here.

For optimal identification of the kinetic parameters, all relevant frequencies of the system should be observable in the output, the measured tissue concentration. This 'identifiability' of the parameters depends on the excitation, the frequencies of the input, as well as on the frequency content of the system, which is determined by the kinetic parameters. When the frequencies of the input are sufficient, such that the system transfers all relevant frequencies for identification to the output, the model is said to be optimal excited. Because in a DCE-MRI study only sampled versions of the true tracer concentration curves can be obtained, only a limited band of frequencies can be studied. Here a tradeoff between temporal and spatial resolution exists. The measured tracer concentration in the artery is (strictly) not the same as the inputs usually considered in system theory and identification, because the input can not be shaped freely by the experimentator, but can only be influenced indirectly by the injection. In this paper the influence of the injection parameters on the arterial frequency content is investigated and, consequently, on the reliability of the kinetic parameter estimation.

The tracer concentration in the blood plasma of the feeding artery (or arteries) of a tumor is often referred to as the arterial input function (AIF). It is possible to measure the AIF in a major artery present in the DCE-MRI measurements [23]. A gamma-variate function can be used to fit to this AIF measurement [15] [16], but this method describes the subject specific relation between injection and arterial concentration insufficiently, because the actual shape of the injection can not be used as input [7] [8]. Strikingly, often a measured AIF cannot be obtained as input from the DCE-MRI measurements. Different methods have been introduced to approximate the concentration curve in the artery, to construct an input necessary for parameter estimation. The most common approach is the use of a fixed bi-exponential AIF model introduced by *Tofts* and *Kermode* [6], which only describes the first pass peak of a contrast agent onwards and neglects any recirculation effects. The large variation op the measured AIF between individuals made this fixed method unreliable, because inter individual differences are not be corrected [22] [18].

A Tracer Distribution Model (TDM) was developed to give a more accurate and flexible description of the relation between the injection and the concentration in the arteries. This model can now provide a physiologic more realistic input for the pharmacokinetic model. Because the TDM uses the injection shape as input and the measured arterial concentration as output, it can predict the arterial concentration curve for any specific injection shape. Also delay times and recirculation effects are incorporated in the model.

Using a simulation study the influence of the injection shape in a DCE-MRI study was investigated. With the help of the Tracer Distribution Model more insight in the relation between the injection shape and the arterial concentration has been gained. Using a system theoretic approach the frequency contents of the concentration curves were analyzed. Also with the help of "Monte Carlo" simulations the influence of the injection on the accuracy of the calculated parameters has been further investigated. The injection was shaped for varying Injection Rate (IR) and Injection Volume (IV) and also aspects like single injection (complete volume injected in a single blow) and multiple injections (the volume divided in multiple parts in time) were investigated. Here the pharmacokinetic parameters were varied within their physiological ranges as exists in normal tissue, metastatic tumor tissue and necrotic tissue. These parameters values determine the dynamics of the pharmacokinetic model.

## Theory and Methods

### *A. Pharmacokinetic Modeling*

We use the pharmacokinetic model proposed by Tofts *et al* to describe the diffusion of an intravascular tracer from the arterial blood plasma $C_p(t)$ to the tumor tissue $C_t(t)$ [3][4]:

$$C_t(t) = v_p C_p(t) + K^{trans} \int_0^t C_p(u) e^{-\frac{K^{trans}}{v_e}(t-u)} du \qquad (1)$$

where $K^{trans}$ is the transfer constant (mL /min /g) of the tracer from the blood plasma to the extravascular extracellular space (EES), $v_e$ is the EES fractional volume (mL /g) and $v_p$ the blood plasma volume per unit volume of tissue (mL /g). $K^{trans}$ can physically be interpreted as the product of $FE$, where $F$ represents the perfusion (or flow) of whole blood per unit mass of tissue and $E$ the initial extraction fraction. Here, $K^{trans}$, $v_e$ and $v_p$ are the tracer kinetic parameters that have to be determined by DCE-MRI measurements.

To inspect the frequency response of the model, equation 1 is transformed into the frequency domain, resulting in:

$$H(w) = \frac{C_p(w)}{C_t(w)} = v_p + \frac{K^{trans}}{iw + K^{trans}/v_e} \qquad (2)$$

where $iw$ is the imaginary frequency component (with $w$ in rad/s), $C_p(w)$ the input and $C_t(w)$ the output in the frequency domain. This results in a first order system with one pole located at $iw = -K^{trans}/v_e$, one zero located at $iw = -(K^{trans}/v_e + K^{trans}/v_p)$ and a direct feedthrough of $v_p$. To illustrate the influence of parameter changes on the frequency spectrum, figure 1 shows the spectra for increasing and decreasing parameter values. Here the modulus of $H(w)$ (in dB) is displayed against the frequency $w$ at a logarithmic scale (a so

called bode plot). The modulus for the lower frequencies are completely determined by $v_e + v_p$ and for the higher frequencies by $v_p$, because of the direct feedthrough of the system.

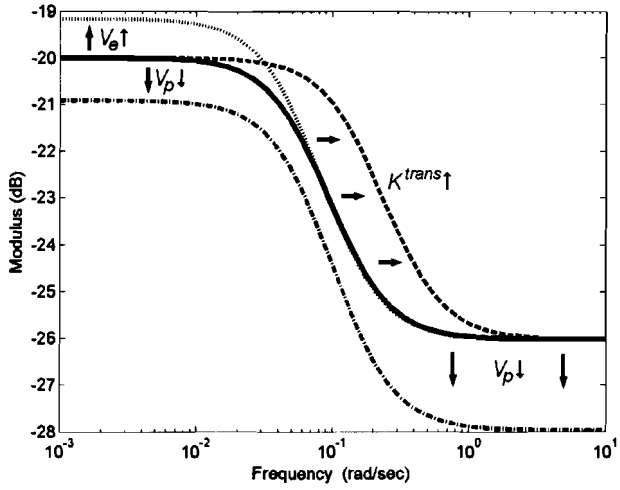


*Figure 1: Influence of the model parameters on the frequency spectrum for increasing $K^{trans}$ (dashed), increasing $v_e$ (dash-dotted) and decreasing $v_p$ (dotted). (Modulus in dB and frequency in rad/sec).*

For identification of the kinetic parameters $K^{trans}$, $v_e$ and $v_p$, the input signal $C_p$ should contain the frequencies relevant for the system dynamics. When such an input excites the system, all relevant frequencies belonging to the system will be transferred to the output $C_t$. This situation is defined as optimal excitation. For the pharmacokinetic system optimal excitation is a big problem because the input can not be influenced directly. The actual input is the injection of contrast agent into the vascular system. When the bolus is injected, it gets dispersed in the distribution through the vascular system, resulting in a decrease of the modulus of all the frequencies. For this reason $C_p$ can only be influenced indirectly by the injection shape. Also the sample frequency determines the frequency content of the signals. The Nyquist theorem states that the maximum frequency $f_{max}$ present in the sampled versions is equal to $f_{max} = f_s/2$, where $f_s$ is the sample frequency. If the signals $C_p$ and $C_t$ contain frequencies above $f_{max}$ these add to, and therefore contaminate, the values of the frequencies below $f_{max}$. This is known as aliasing.

The ratio $K^{trans}/v_e$ determines the cut-off frequency at which the modulus is 3 dB below the steady state gain (gain at $w$=0). When $K^{trans}$ increases the cut-off frequency shifts to the right (see figure 1), which makes the relevant frequency band greater. Now first of all, the sample frequency must be higher to include all relevant frequencies and second $C_p$ must contain higher frequencies to optimal excite the system. These two aspects can introduce an error. When $v_e$ increases the cut-off frequency shifts to the left and the steady state gain increases. Now a $C_p$ signal with a less high frequency content could be sufficient to optimally excite the system. Also the sample frequency could be lower to include all relevant frequencies. The increase of $v_p$ will also increase the steady state gain, which enhances the response for lower frequencies [21].

*B. The Injection Shape*

The injection can be varied with respect to the speed of injection, the injection rate (IR), and the volume of the contrast agent, the injection volume (IV). These injection parameters determine the shape of the injection, which should be within clinically acceptable limits to not damage the injection site (the antecubital vein). For this reason a maximum for both for the injection rate and injection volume exists.

When the injection volume is not injected at once, but divided in different fractions in time, it is called multiple injections. In figure 2 a single (2a) and a double (2b) injection are shown for the injection rate against time. The injection has the shape of a trapezoid because an automated pump is used as injector for the DCE-MRI measurements. The pump has an adjustable constant maximal injection rate, with a rising and a falling slope. The total surface under the trapezoids corresponds to the injection volume, which is the same for all the examples displayed in figure 2. Further with multiple injections, it is possible to vary the number of injections and timing between these injections.

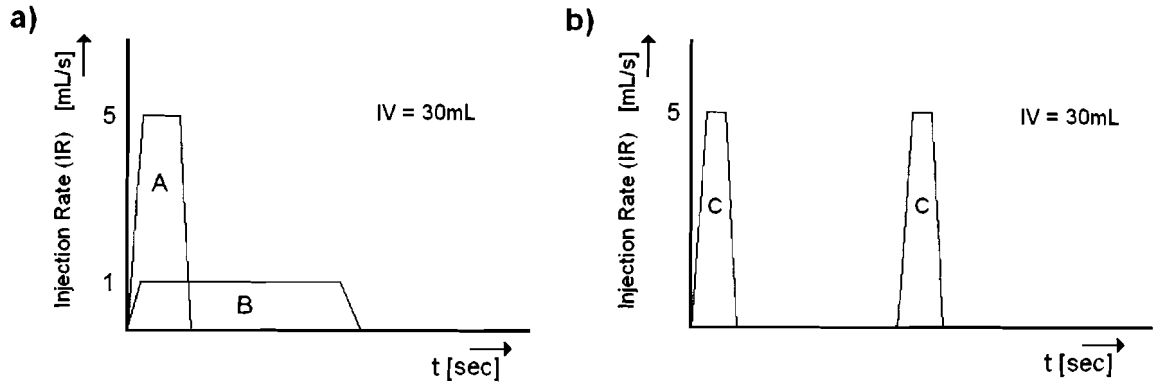


*Figure 2: Schematic Representations of possible injection shapes. Single Injection (a): Shape **A** with injection rate (IR) of 5mL/s and **B** with 1mL/s, and multiple injections (b) with shape **C** with an injection rate of 5mL/s and is divided in two separate injections. The injection volume (IV) is 30mL.*

To optimize the shape of the injection the energy of the signal can be calculated. This can be obtained by *Parseval's theorem*, which states that the total energy contained in a signal $f(t)$ across all time $t$ is given by:

$$E_f \triangleq \int_{-\infty}^{\infty} |f(t)|^2 dt \triangleq \frac{1}{2\pi} \int_{-\infty}^{\infty} |F(w)|^2 dw \qquad (3)$$

The theorem says that the energy of a time signal can be calculated not only in the time domain, but also in the frequency domain, by integrating the magnitude squared spectrum [X]. The signal with the most energy will contain the highest frequency content, and is expected to be optimal for excitation. To illustrate the dependence of the injection shape on the energy of that signal, in figure 2 example injections are shown.

For the single injection (2a), both injection shape *A* and *B* use the same injection volume (30mL), so the area under the curve is the same for both curves. However, shape *A* is injected with 5mL/s and shape *B* with 1mL/s. Using *Parseval's theorem* the energy of injection shape *A* is higher then shape *B* because the amplitude is squared. In this example the energy of shape *A* is 142 and of shape *B* is 30, if the rising and falling slope is set to 1sec. This is a big difference, which when transformed to the frequency spectrum will result in a much higher frequency content of shape *A* then *B*, even a proximally 5 times as high. To optimally shape the injection, so it contains the most energy, the largest rate with the largest volume is the optimum.

When multiple injections are used, the volume (also 30mL) is injected in multiple parts in time, illustrated in figure 2b. The total surface under the trapezoids is the same as for the single injection. Again, using theorem 3 the energy of the signal can be calculated. Due to the extra rising and falling slope, the energy is less the single injection case. Now the total sums up to 133, instead of the 142 of the single injection (shape *A*). This loss of energy for multiple injections (at the same IR and IV) is increasingly for the number of injections. The further illustrate this effect, a comparison of the rectangular situation (the ideal case) with the trapezium shape is described in appendix A, where both the energy as the frequency spectrum is compared.

*C. Tracer Distribution Model*

The distribution of a contrast medium through the vascular system is complex. The injected bolus travels from the injection site (the antecubital vein) through the vena-cava to the heart's right atrium and ventricle. Then the bolus will travel through the lungs back to the heart. The left ventricle will pump the bolus into the aorta, from which it will split up into the various arteries. A part of the tracer molecules will pass through the feeding artery (or arteries) of the tumor and will diffuse into the tumor tissue. Afterwards the bolus will recirculate back to the heart. After a second pass through the vascular system, the contrast agent will be homogeneously distributed throughout the vascular system and will slowly be excreted by the kidneys.

The Tracer Distribution Model (TDM) was developed to simulate the distribution of a tracer through the vascular system. In figure 3 the model is shown, were the injection is the input of the model, indicated with $u$, and the arterial blood plasma concentration the output, indicated with $C_p$.

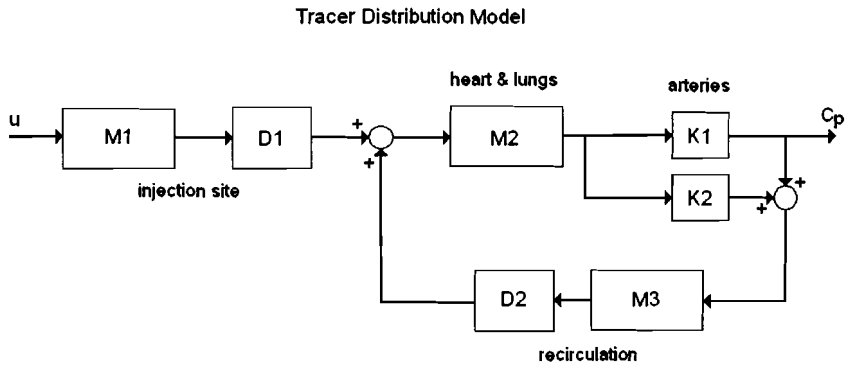


*Figure 3: The input-output Tracer Distribution Model, u is the injection shape and $C_p$ the arterial blood plasma concentration.*

With the sub-models:

$$M1 = \frac{B_{01}}{s^2+A_{11}s+A_{01}} \quad (4)$$

$$M2 = \frac{B_{22}s^2+B_{12}s+B_{02}}{s^2+A_{12}s+A_{02}} \quad (5)$$

$$M3 = \frac{B_{03}}{s^2+A_{13}s+A_{03}} \quad (6)$$

$$D1,D2 = \text{Time Delays} \quad (7)$$

$$K2 = K1\text{-}1 \text{ (K1,K2 are gains)} \quad (8)$$

The sub-models M1, M2 and M3 describe the smoothing the injection undergoes in the vascular system. The smoothing at the injection site is modeled with M1, the heart and lungs with M2 and the recirculation with M3. The delay time between injection and measurement location is described with D1 and the recirculation time with delay D2. Also a fraction of the tracer will pass around the measurement location through other arteries, which is described with the gains K1 and K2. The transfer function coefficients (parameters $A$ and $B$) of equation 3-5 have no physiologic meaning and are for that reason not important to classify. For our use is only the predicted output of the TDM, the arterial blood plasma concentration, of interest, not the individual parameters of the TDM.

*D. Parameter Identification*

Now the mathematical model structures have been defined, the estimation of the parameters of interest ($K^{trans}$, $v_e$ and $v_p$) can be investigated. The process to estimate the parameters of a model based on the observed input and output data is called 'identification'. The 'identifiability' of the parameters depends on the model structure, the spectral properties of the system and the experimental conditions, like sample time, signal-to-

noise level and the experiment duration. The spectral properties, which reflect the dynamics of the system, depend on the values of the kinetic parameters (see equation 2).

*M* is defined as the model-set of all models for the possible range of the parameters. When it is assumed that the real system *S* exists in the model-set *M*, as defined (*S*∈ *M*), all dynamics of the real system *S* can be described within the model-set *M*. When the input and output data have been acquired, the parameters can be estimated. When the 'true' parameter values of the real system *S* are defined as $\theta^{true}$ , the best estimates of these values can be found by tuning the model parameters $\tilde{\theta}$ such that the model output optimally describes the acquired measurement data. It is assumed that the model will equal the real system for $\tilde{\theta} = \theta^{true}$ . In our identification setup there are two parameters sets, the kinetic parameters indicated with $\theta_{kin} = (K^{trans}, v_e, v_p)$ and the parameters of the tracer distribution model, indicated with $\theta_{TDM}$ . Notice that in our setup the parameters of the TDM are not of importance, we are only interested in the kinetic parameters. Only the input-output behavior of the TDM is of interest in our setup.

The standard least squares (LSQ) is a commonly used estimator for the calculation of the kinetic parameters in a DCE-MRI measurement [X] [X]. The LSQ estimation for the parameters $\theta_{kin}$ , denoted by $\hat{\theta}_{kin}$ , can be found by minimizing the cost function $V_1$:

$$\hat{\theta}_{kin} = \arg\min_{\tilde{\theta}_{kin}} V_1 \tag{9}$$

with the cost function $V_1$ denoted by:

$$V_1 = \frac{1}{2\sigma_{\varepsilon_2}^2} \sum_{i=1}^{N} \left( C_{tm}(i) - \tilde{C}_t(\tilde{\theta}_{kin}, C_{pm}(i), i) \right)^2 \tag{10}$$

where $C_{tm}$ is the measured tumor tissue signal, $\sigma_{\varepsilon_2}$ the standard deviation of the model residuals for $C_t$ (the error $\varepsilon_2$) and *N* the number of samples. The output of the pharmacokinetic model is denoted by $\tilde{C}_t$ for the tuned parameters $\tilde{\theta}_{kin}$ and the corresponding $C_{pm}$. An optimization algorithm will try to find a minimum of the cost function of equation 9. The standard deviation of the noise is not always known beforehand. However, this does not influence the estimation because it is only a multiplication factor of equation 10 and does not change the location of the minimum of the cost function.

The same standard least squares can be used to estimate the parameters $\theta_{TDM}$ of the TDM, minimizing the cost function $V_2$:

$$\hat{\theta}_{TDM} = \arg\min_{\tilde{\theta}_{TDM}} V_2 = \arg\min_{\tilde{\theta}_{TDM}} \frac{1}{2\sigma_{\varepsilon_1}^2} \sum_{i=1}^{N} \left( C_{pm}(i) - \tilde{C}_p(\tilde{\theta}_{TDM}, u(i), i) \right)^2 \tag{11}$$

where $C_{pm}$ is the measured tumor tissue signal and $\sigma_{\varepsilon 1}$ is the standard deviation of the model residual on $C_p$. The injection shape is denoted by *u*. The best estimation of the TDM for the arterial plasma concentration $\hat{C}_p$ can now be calculated with:

$$\hat{C}_p(i) = C_p(\hat{\theta}_{TDM}, u(i), i) \tag{12}$$

*E. TDM Selection*

The tracer distribution model was selected based on DCE-MRI measurements, also used in the study of De Lussanet *et al.* [X]. DCE-MRI was performed on 17 patients with a conventional clinical MRI scanner at 1.5 Tesla (Intera, Philips, Best, The Netherlands), with a five-element cardiac phased array coil. DCE-MRI included six precontrast T1-weighted measurements (3D fast-field echo, TR 8.0 ms, echo time 3.9 ms, 10

axial slices [slice thickness, 8 mm], field-of-view 290 _ 290 mm, matrix 128 _ 128) with different flip angles (FAs) (2°, 5°, 10°, 15°, 25°, and 35°) to determine the T1 relaxation time in the blood and tissue before the contrast agent arrives, on a pixel-by-pixel basis. This was followed by the dynamic contrast-enhanced series using the same sequence but with an FA of 35° only (250 scans of 2.4 s), for a total duration of 10 min. Gadopentetate dimeglumine (Schering AG, Berlin, Germany; 0.15 mmol/kg body weight) was injected intravenously (3 mL/s) and flushed with 15 mL saline (3 mL/s) at the start of the eighth dynamic scan. Local T1 relaxation rates (in this case 4.1 [1/mMs]) of the precontrast time-averaged images and contrast-enhanced image signal intensity time courses were used to determine the concentrations of contrast medium in the blood plasma (common femoral arteries) and tumor. An experienced gastrointestinal radiologist has defined the tumor volume region of interest on the T1-weighted images.

For the selection of this tracer distribution model, different model structures have been examined. Black box models where tried, but with low-order models (<20 order) the delays were hard to estimate, and for high order models (>20 order) the noise was made part of the dynamics. For this reason a gray model structure was selected, where the structure of the model (the layout of the sub-models) was based on knowledge of the real physiology, the vascular system. The actual complexity of the sub models *M1*, *M2* and *M3* (the number of *A* and *B* parameters of equation 4-6), were selected based on the white noise test of the residuals. This test states that if the selected model corresponds with the "real system" (the vascular system), the residuals show whiteness and a Gaussian distribution, and all the dynamics of the "real system" is sufficiently described. Using equation 11 the cost-function $V_2$ was minimized to find the best estimates for $\hat{\theta}_{TDM}$ parameters. Then, using equation 12, the 'best' prediction of $\hat{C}_p$ of a single DCE-MRI measurement was generated.

Because the models *M1*, *M2* and *M3* have multiple degrees of freedom the model is not identifiable giving only $C_p$ measurements, meaning that there exists no unique set of the parameters for a single $C_p$ curve. For this reason multiple solutions are possible which will result in the same input-output dynamics of the model. This is not a problem because the *A* and *B* parameters are not of importance, only the input-output dynamics. If a Padé approximation is used for the time delays, the TDM is linear [X]. Now the TDM will be a complex, but passive linear filter, meaning that only energy is dissipated.

*F. Simulation Setup*

One, not selected in particular, DCE-MRI study was used for further analysis (see left figure 4). This study was conducted with an injection volume of 45mL 0.5M Gd-DTPA, injected with an automated pump at an injection rate of 3mL/s. The duration of the rising and falling slope of the injection shape was set to 1 sec, corresponding with the specification of the pump. Using the injection $u$ (as defined above), the 'best' prediction for this measurement of $\hat{C}_p$ was calculated using equation 11-12 and resulted in the following TDM parameters $\hat{\theta}_{TDM}$ : $A_{01} = 0.083$, $A_{11} = 0.265$, $B_{01} = 0.043$, $A_{02} = 1.451$, $A_{12} = 22.803$, $B_{02} = 0.535$, $B_{12} = 0.516$, $B_{22} = 0.726$, $A_{03} = 0.312$, $A_{13} = 15.525$, $B_{03} = 0.642$, $D1 = 17.091$, $D2 = 13.730$ and $K1 = 0.390$.

Now the TDM was 'fixed' with the parameters $\hat{\theta}_{TDM}$ , the arterial concentration $C_p$ could be simulated for any injection shape, using equation 12. This shape however, must be within the clinical ranges usable for humans: the Injection Rate (IR) = 0.5-5 ml/s and the Injection Volume (IV) = 5 – 45 ml of 0.5M Gd-DTPA. Simulations were conducted to analyze the influence of the injection on the frequency spectrum of the arterial concentration (to investigate optimal excitation) for both a single and multiple injections. The frequency ranged from $10^{-3}$ to $10^{3}$ Hz. To sufficiently include all the lower and higher frequencies, the duration of the experiment was set to 30 minutes with a sample rate of 100 Hz. A moving average filter was used to smooth the resulting frequency spectra to make the spectrum figures more readable.

To investigate the influence of the injection shape on the accuracy of the parameters, "Monte Carlo" simulations were performed to elucidate the conclusions from the spectrum analysis. With help of the pharmacokinetic model (equation 1 and 2) the tissue concentration response of the arterial concentration can be simulated. Here a large number of simulated (synthetic) tissue concentration datasets are added with a random white Gaussian noise with zero mean. From these "synthetic data sets" the parameters were estimated, which resulted in a distribution of parameter values. From this distribution the properties can be examined. The "Monte Carlo" method delivers accurate results as long as a large number of simulations are performed. The duration of the acquisition was set fixed to 10 minutes and sample rate was set fixed to 1 sec,

this because these aspects are not under study. The signal-to-noise ratio (SNR) was set to 10, resulting in a noise of 10% of the tissue concentration. The number of simulations was set to 1000 for each condition, the injection shape and the $K^{trans}$ value. The range of the parameters was set to: $K^{trans}$ = 0.001 – 0.5 mL/min/g, $v_e$= 0.01-0.5 mL/g and $v_p$= 0.01 – 0.5 mL/g.

The parameter estimation was implemented in MATLAB©, where the function *lsqnonlin* was used as least squares algorithm. SIMULINK© and *lsim* were used to generate the concentration curves. Both the parameters of the TDM and of equation 1 where found with this method. The Levenberg-Marquart optimalization was used, the relative and absolute tolerance were set to 1e-8 and the maximal number of iterations for the TDM and the pharmacokinetic model were set to 500. There were no constraints set to the parameters of equation 1, but only the lower constraints of the TDM were set to zero to ensure the model is stable. By means of the "Monte Carlo" method the inaccuracy of the parameter estimation can be analyzed, therefore the bias $\left((\overline{\hat{\theta}} - \theta_t)/\theta_t\right)$, the estimated standard deviation $\left(\hat{\sigma}_{\hat{\theta}}\right)$ and the estimated relative error $\left(\hat{\sigma}_{\hat{\theta}}/\overline{\hat{\theta}}\right)$ of the parameters were calculated. Here the $\theta_t$ represents the true parameter value and $\overline{\hat{\theta}_t}$ the mean of the estimated parameter.

## Results

### *A. Single Injection*

To illustrate the fitting capacity of the TDM, in figure 4 two examples are shown of two different DCE-MRI measurements. Left a common AIF curve without visible recirculation effects and right a less common, but possible, AIF curve with clearly visible recirculation peak. These are measurements of different patients at different locations. The second curve is shown to illustrate the recirculation capabilities of the tracer distribution model. Here also D1 and D2 of the TDM are shown to illustrate the delay times in the model. The first curve (left) will be used for further analysis.

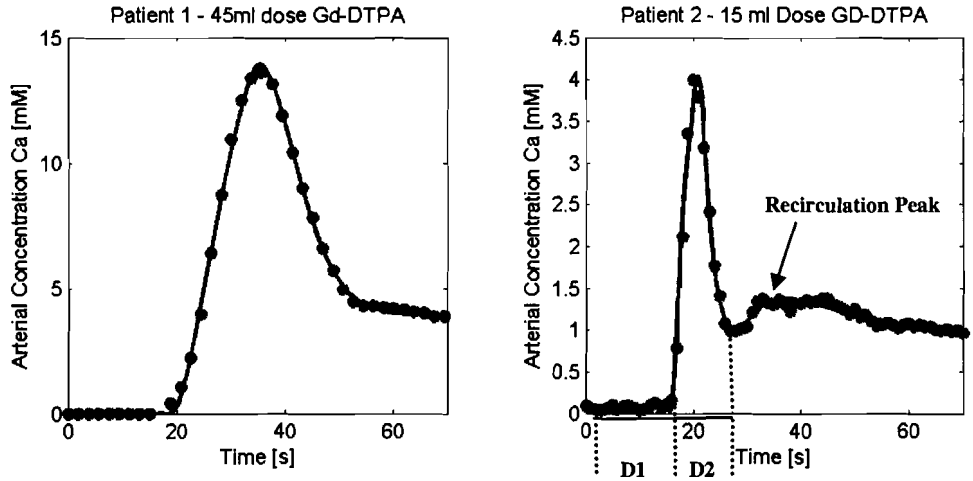


*Figure 4: Examples of two TDM fits of DCE-MRI measurements, from different patients at different locations. The dots represent the measurement points and the solid line the fitted curve of the TDM. Left: patient 1 measurement without visible recirculation effects. Right: patient 2 measurement with a visible recirculation peak.*

With the help of the fixed TDM model, the arterial concentration curves from different injection shapes can be calculated. The results are shown in figure 5, where the injection shapes are displayed in the left figures and the arterial response are shown in the right figures.

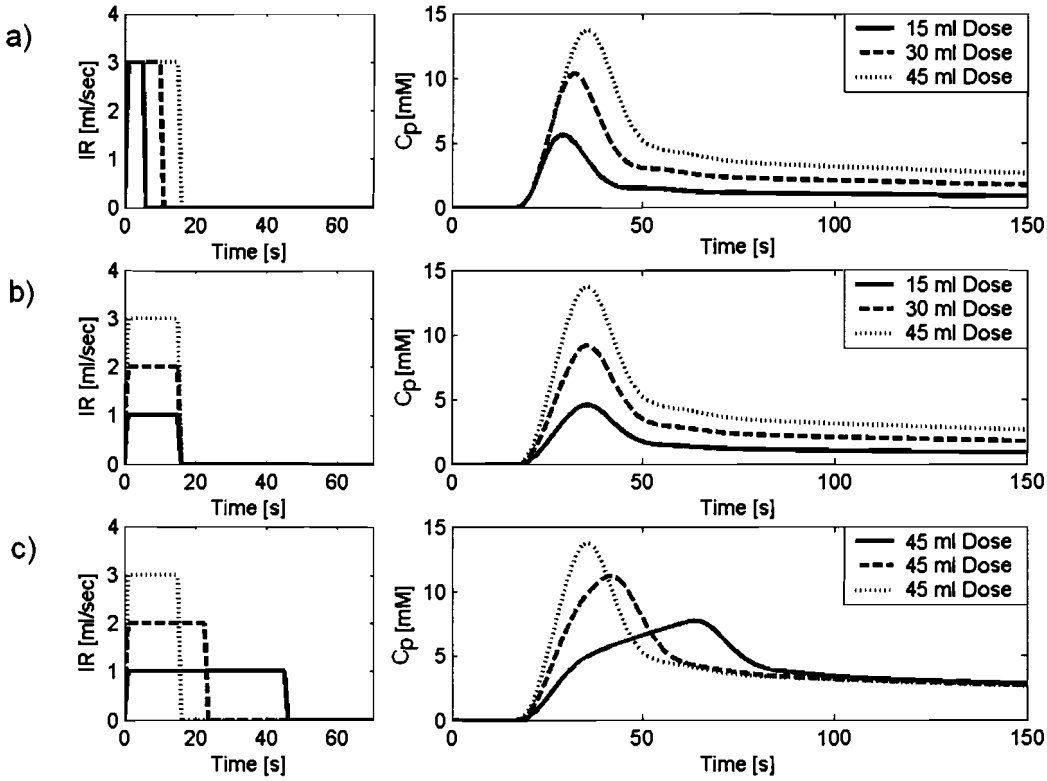


*Figure 5: Simulations with a fixed TDM for various injection shapes. Left: injection shape with the injection rate (IR) against time, right: arterial concentration ($C_p$) against time for (a) varying injection volume, (b) varying injection rate and injection volume and (c) varying injection rate.*

In figure 5a the injection volume has been varied at a constant injection rate, which results in a longer injection duration for a larger volume (left figure). An increase in volume results in a larger concentration peak which is shifts towards the right, thus the maximum concentration will be reached in a later point in time (right figure). The first part of the rising slope of the three curves is identical. In figure 5b both the injection volume and the injection rate is varied. Because this is a linear multiplication of the input signal, consequently the arterial concentration also increases linear, as can be expected by a linear model. The arterial concentration peak is for all the inputs at the same point in time. Figure 5c shows the response of the TDM when only the injection rate is varied and the injection volume is kept constant. This results in a shorter injection duration for a faster rate. For increasing rate the concentration peak will shift to the left, earlier in time, and will have a higher maximum.

Next, the frequency spectra of the concentration curves can be investigated. The results are shown in figure 6, where the subplot 6a shows the injection shape, 6b the arterial concentration curve and 6c the resulting spectrum of the concentration curve at a logarithmic scale. Only the 15mL and 45mL injection volume (IV) with an injection rate (IR) of 1 and 5mL/s are shown to keep the figure readable.

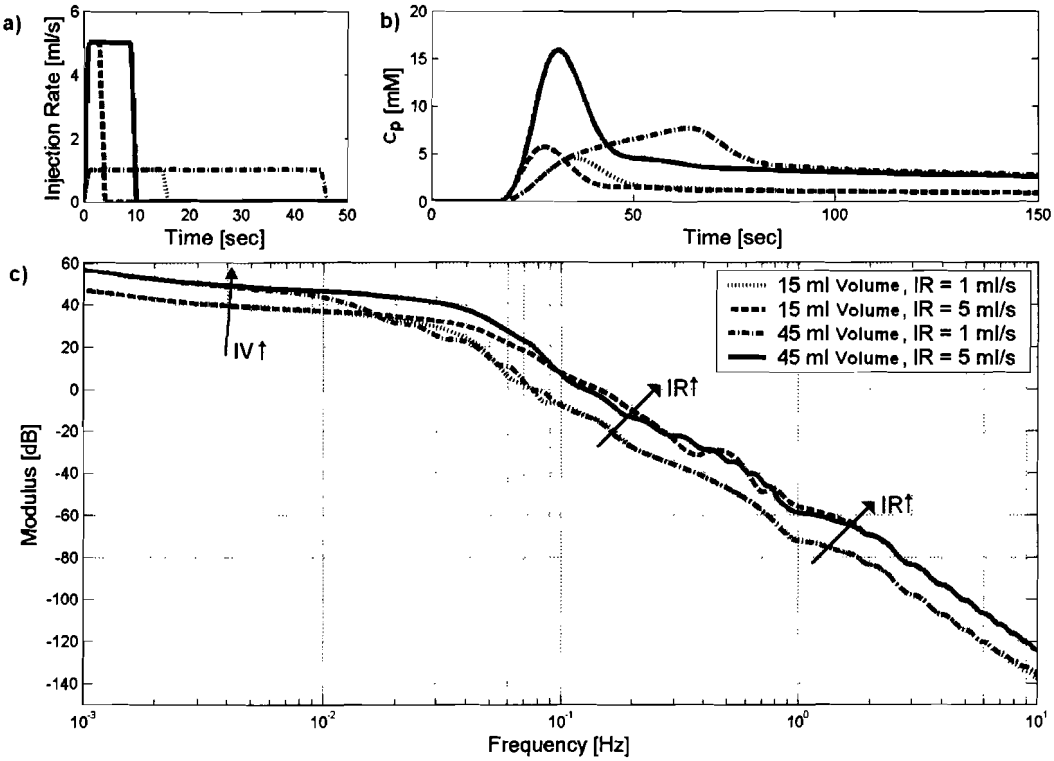


*Figure 6: Single injections with injection volumes of 15ml and 45ml and injection rates of 1ml/s and 5ml/s. a) the injection rate, b) the arterial concentration and c) the spectra of the arterial concentration. These spectra are smoothed to keep the figure readable. Arrows indicate the increase in volume and rate.*

Figure 6c shows that the injection volume only affects the modulus of the lower frequencies (below 0.02 Hz) for a maximum of 15 dB. The injection rate influences the modulus of the higher frequencies, the range from 0.01 Hz and higher, where the increase is maximal 15 dB. These spectra are smoothed to keep the figures readable. Because the sample rate of a DCE-MRI measurement is always above 100 sec, the influence of the injection rate is measurable. The influence of the injection volume is always measurable because the whole lower spectrum is affected.

The influence of the injection volume on the excitation is for all possible system dynamics, determined by the kinetic parameters, very relevant. Because the scales are plotted logarithmic, the illusion is created that the IV influences a large range. This is false because this is actually a very small range of frequencies, but very relevant for identification. For high values of $K^{trans}$ the location of the pole and the zero shifts to the right. Now the influence of the injection rate is increasingly important, because higher frequencies are relevant for identification.

One important aspect can be noticed. There is no tradeoff between one shape being optimal for the low frequencies and another for the high frequencies, as one might expect. When the highest injection volume is injected as fast as possible, this signal will contain the highest energy, and is the best excitation for the whole frequency spectrum. Because of the dissipation of energy through the TDM, energy from the injection shape will be lost in the transfer. But still, the injection with the highest energy will transfer the most energy to the arterial concentration.

*B. Multiple Injections*

To investigate multiple injections, the injection is divided into multiple parts in time. For fair comparison the injection volume and injection rate are kept constant at 45mL and 3mL/s respectively.

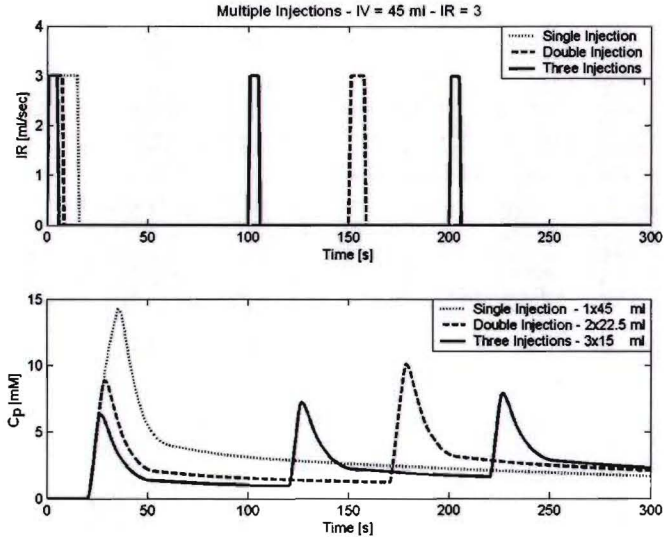


*Figure 7: Simulations with the TDM with multiple injections. Above: injection rate (IR) for a single, double and triple injection. Below: corresponding simulated arterial concentration ($C_p$) against time.*

In figure 7 the different profiles are shown for a single, a double and a triple injection. Consequently, the arterial concentration displayed multiple, but lower, peaks. To illustrate the effect of the number of injections on the frequency spectrum, figure 8 is shown.

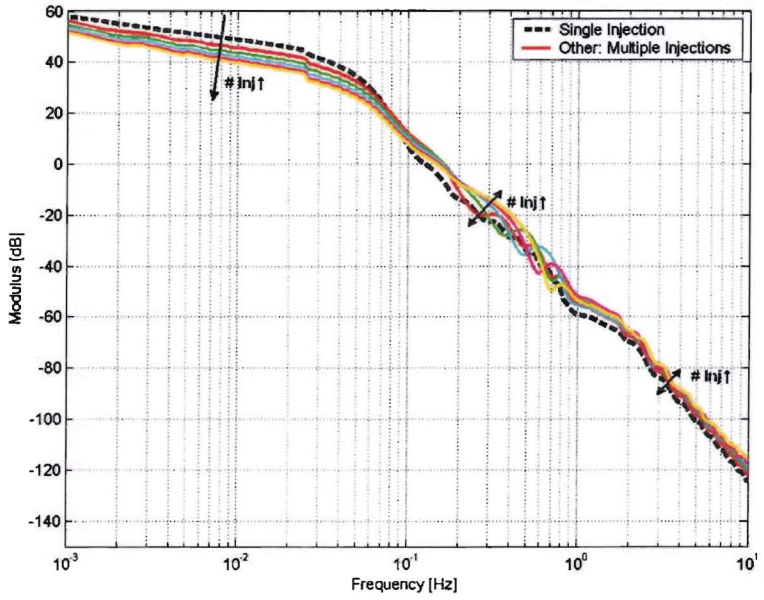


*Figure 8: Frequency Spectrum of multiple injections. Dashed single injection and colored multiple injections, red double, green triple, blue four, pink five and yellow six injections. The figure is smoothed to keep it readable. Arrows show the increasing number of injections.*

For an increasing number of injections a decrease can be seen for the modulus of the lower frequencies, as illustrated in figure 8. Here a maximum of 6 separate injections are shown. For an increase of the number of injections, only small parts of the higher frequencies are affected, where the deviation with the single injection is small. More than 6 injections do not change the spectrum much, and are for that reason not shown.

Important to notice, is that here a tradeoff exists, as proven with the *Parseval's Theorem*. The energy of a single injection (with the same IV and IR) is a proximally the same as for the multiple injections (besides the lost due to the rising and falling slope). The loss of the moduli of the lower frequencies will mean an increase of the moduli of the higher frequencies. Because the lower frequencies are crucial for identification, multiple injections will decrease the excitation of the pharmacokinetic model.

### *C. The "Monte Carlo" simulation study*

The influence of the injection rate and the injection volume on the estimation of the parameters was analyzed using a "Monte Carlo" simulation study. Table 1 and 2 show the results, where the bias and relative error of $K^{trans}$ is displayed for different system dynamics (varying $K^{trans}$ true), where table 1 shows the results for varying injection rate and table 2 for varying injection volume. All other conditions were kept constant, like SNR, sample time and $v_e$ and $v_p$ values.

*Table 1: Results for varying Injection Rate (IR)*

| | | $K^{trans}$ | | $v_e$ | | $v_p$ | |
|---|---|---|---|---|---|---|---|
| IR (ml/s) | True $K^{trans}$ (ml/min/g) | Bias (%) | Relative Error (%) | Bias (%) | Relative Error (%) | Bias (%) | Relative Error (%) |
| 1 | 0.01 | -0.0186 | 10.0809 | 1.8938 | 6.3437 | -0.3565 | 2.4597 |
| | 0.1 | 0.3679 | 11.9851 | 0.2108 | 4.8917 | -0.2097 | 5.1547 |
| | 0.5 | 12.2720 | 43.7780 | 4.1118 | 22.8445 | -4.5733 | 23.0704 |
| 3 | 0.01 | 0.2637 | 8.4218 | 0.7306 | 4.8062 | -0.0094 | 2.0069 |
| | 0.1 | -0.4756 | 8.2974 | 0.0290 | 3.1316 | 0.0235 | 2.9081 |
| | 0.5 | 2.2347 | 19.8882 | 0.2516 | 8.2853 | -0.3170 | 8.6235 |
| 5 | 0.01 | -0.1416 | 6.8771 | 0.3310 | 5.4126 | 0.0957 | 1.6857 |
| | 0.1 | 0.6749 | 7.7131 | -0.0385 | 3.1166 | -0.1480 | 2.8745 |
| | 0.5 | 2.1156 | 14.8792 | 1.0339 | 6.5045 | -1.0112 | 6.7767 |

*Results of the bias and relative error form the computed kinetic parameters, for varying Injection Rate (IR) and the true $K^{trans}$ (mL /min /g). The true values of parameters were kept constant at: $v_e$=0.05 (mL /g) and $v_p$=0.05 (mL /g). The sample time and SNR were kept constant at 1 sec and 10 respectively. The Injection Volume (IV) was set to 15 mL.*

*Table 2: Results for varying Injection Volume (IV)*

| | | $K^{trans}$ | | $v_e$ | | $v_p$ | |
|---|---|---|---|---|---|---|---|
| IV (ml) | True $K^{trans}$ (ml/min/g) | Bias (%) | Relative Error (%) | Bias (%) | Relative Error (%) | Bias (%) | Relative Error (%) |
| 15 | 0.01 | 5.3007 | 22.0116 | 3.8944 | 19.7187 | -0.3339 | 5.3408 |
| | 0.1 | 7.1276 | 20.9125 | 0.1422 | 8.0851 | -1.2733 | 7.2400 |
| | 0.5 | 5.3821 | 37.0824 | 0.3820 | 18.0493 | 0.1702 | 19.1215 |
| 30 | 0.01 | 0.9912 | 13.4157 | 2.3202 | 9.3458 | -0.0644 | 3.0803 |
| | 0.1 | -1.0125 | 10.8810 | 0.0616 | 4.3661 | 0.2765 | 3.9118 |
| | 0.5 | 4.3179 | 23.5492 | 1.6051 | 10.7178 | -1.6613 | 11.1902 |
| 45 | 0.01 | 0.4207 | 8.0777 | 0.6257 | 5.4824 | -0.0918 | 1.9151 |
| | 0.1 | -0.4953 | 7.6944 | 0.2235 | 2.9060 | 0.2065 | 3.0032 |
| | 0.5 | 0.9944 | 19.0295 | 0.6585 | 8.9951 | -0.6792 | 9.1923 |

*Results of the bias and relative error form the computed kinetic parameters, for varying Injection Rate (IR) and the true $K^{trans}$ (mL /min /g). The true values of parameters were kept constant at: $v_e$=0.05 (mL /g) and $v_p$=0.05 (mL / g). The sample time and SNR were kept constant at 1 sec and 10 respectively. The Injection Rate (IR) was set to 3 mL/s.*

Both table 1 and 2 show for an increase of the true $K^{trans}$, an increase of the bias and relative error for all the parameters. Table 1 shows that an increase of the injection rate improves the accuracy of the parameters. For a high perfusion rate, a high $K^{trans}$, a great improvement on the bias and relative error can be seen. The injection volume has also a big influence on the accuracy, as shown in table 2. The bias and relative error of $K^{trans}$ is higher, then for the $v_e$ and $v_p$ parameters, which indicates that the $K^{trans}$ is more difficult to accurately determine, then the $v_e$ and $v_p$ parameters. From table 1 can be seen that for high values of $K^{trans}$ true the injection rate is increasingly important. For the low values this is much less and, a less high frequent arterial signal is sufficient. The injection volume however (see table 2) is for all values of $K^{trans}$ important, which again shows the importance of the low frequencies.

To further illustrate the influence of the injection rate and injection volume, in figure 9 the bias and relative error is shown for the parameter $K^{trans}$ for varying injection rate and injection volume.

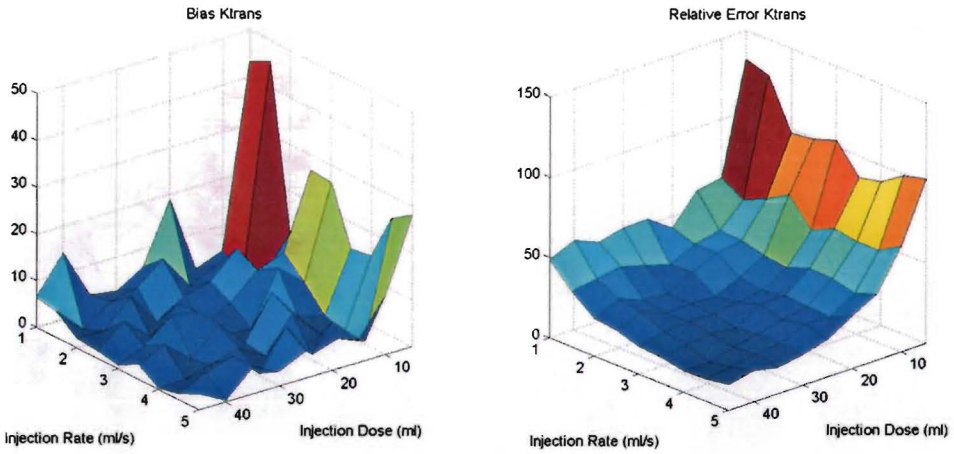


*Figure 9: Influence of Injection Rate and Injection volume of a single injection on the accuracy of $K^{trans}$: the absolute bias (left figure in %) and the relative error (right figure in %). The true parameters were kept constant at: $K^{trans}$ =0.5 (mL/min/g), $v_e$=0.05 (mL/g) and $v_p$=0.05 (mL/g). The sample rate and SNR were constant at 1 sec and respectively 10.*

As figure 9 shows, the bias and relative error is the smallest for the highest injection rate and the highest injection volume. A large error can be expected when a small volume is used (< 15 mL). Also a small rate increases the error, below 2 mL/s the accuracy decreases rapidly. When, clinically, a small dose must be applied, the rate should be as high as possible. Also, when a small injection rate must be applied, the dose should be as high as possible.

To investigate the influence of multiple injections, table 3 and 4 shows the bias and relative error of the kinetic parameters for varying number of injections, for a 15mL volume (table3) and a 45mL volume (table 4).

*Table 3: Results for Multiple Injections*

| Number of Injections | $K^{trans}$ Bias % | $K^{trans}$ Relative Error % | $v_e$ Bias % | $v_e$ Relative Error % | $v_p$ Bias % | $v_p$ Relative Error % |
|---|---|---|---|---|---|---|
| 1 | 5.5594 | 34.7513 | 2.1752 | 16.8122 | -1.2871 | 17.3009 |
| 2 | 2.1574 | 46.9790 | 2.6819 | 25.7186 | -1.0750 | 22.4965 |
| 4 | -10.8459 | 69.2336 | 12.0699 | 38.4918 | -9.1000 | 32.6263 |
| 6 | -13.5481 | 77.2755 | 15.5764 | 43.5624 | -11.2152 | 34.9923 |

*Results for the computed bias and relative error of $K^{trans}$, $v_e$, $v_p$ when estimated with multiple injections. The parameters were set to: $K^{trans} = 0.5, v_e = 0.05, v_p = 0.05$. The sample time and SNR were kept constant at 1 sec and respectively 10. The injection volume was set to 15 ml at an injection rate of 3mL/s.*

*Table 4: Results for Multiple Injections*

| Number of Injections | $K^{trans}$ Bias % | $K^{trans}$ Relative Error % | $v_e$ Bias % | $v_e$ Relative Error % | $v_p$ Bias % | $v_p$ Relative Error % |
|---|---|---|---|---|---|---|
| 1 | 6.8394 | 17.8921 | 2.8512 | 7.7429 | -2.9471 | 8.6367 |
| 2 | 5.2357 | 18.9639 | 3.0562 | 7.5086 | -3.0970 | 8.1907 |
| 4 | 4.3465 | 25.8062 | 2.6239 | 11.0531 | -2.6999 | 11.9166 |
| 6 | 5.8269 | 30.7080 | 3.0289 | 12.9889 | -2.8998 | 13.8742 |

*Results for the computed bias and relative error of $K^{trans}$ when estimated with multiple injections. The parameters were set to: $K^{trans} = 0.5, v_e = 0.05, v_p = 0.05$. The sample time and SNR were kept constant at 1 sec and respectively 10. The injection volume was set to 45 ml at an injection rate of 3mL/s.*

For an increasing number of injections, an increase of the bias and relative error can be seen for all the kinetic parameters. Here, again the importance of the lower frequencies are displayed. The reduction of the moduli of the lower frequencies, as shown in figure 8, had a large influence on the accuracy. When the lower frequencies are sufficiently represented, because of the injection volume of 45mL, the multiple injections

have a smaller effect on the accuracy. But still is the single injection favorable. Also a large number of injections were investigated (until 20), but again no improvement was gained, the results only became increasingly worse. Also the timing between the injections had no effect (results not shown).

**Discussion**

This study was performed to investigate the influence of the injection parameters on the reliability of the estimation of the pharmacokinetic parameters representing endothelial permeability, and consequently, to optimize the experimental settings for DCE-MRI. As could be expected, had the energy content of the signal, which can be calculated with *Parseval's Theorem*, a large influence on the accuracy and reliability of the kinetic parameters. Also the frequency analyses and the "Monte Carlo" simulations showed a large influence of both the injection volume and injection rate on the bias and relative error of the kinetic parameter estimates. A larger injection volume increased the modulus of the arterial concentration for lower frequencies (see figure 6), but did not affect the higher frequencies. This improvement of the lower frequencies was, as expected, of great importance for the identification (see table 1 and 2 and figure 9). The injection volume should always be larger than 15mL, otherwise the arterial curve cannot be distinguished from the noise which results in an inaccurate estimation (see figure 9). An increase of the injection rate had also a large influence on the frequency spectrum, and now the modulus of the higher frequencies (above 0.01 Hz) had increased. Table 1, 2 and figure 10 show a large influence of the injection rate on the identifiability of the parameters. Low injection rates (below 2 mL/s) should be avoided, otherwise a large inaccuracy must be expected. From figure 10 one might get the impression that the injection volume had a bigger influence than the injection rate, which can be deceiving because of the chosen range because, very small injection rates (below 1 ml/s) also showed a large increased of the bias and relative error. Therefore, for optimal results both the injection rate and the injection volume should be as high as possible. Previous studies also indicated the best excitation for the highest injection rate [10][21], but they did not thoroughly investigated the actual shape of the injection (including also the volume).
Injecting the volume in multiple parts had also an effect on the spectrum. Here a significant tradeoff between a decrease in the lower frequencies and an increase in the higher frequencies, but energy was lost due to the extra rising and falling slope (*see Parseval's Theorem).* The lower frequency range is very essential for good identification, therefore a multiple injection is not recommended, especially because there is no apparent increase for the higher frequencies. Also the simulation study emphasized these findings (see table 3, 4). For this reason a single injection is favorable to yield the best arterial concentration input for the pharmacokinetic model. Also other injection shapes, than the trapezium, where investigated. It was possible to increase frequencies by pulsating the injection at a defined frequency, but this was only for a small region and did not improve the results in the "Monte Carlo" study.
The injection shape used in this study resembled a trapezium shape, because this was the injection profile of the automated pump used for our DCE-MRI experiments. Using this automated pump, it is clinically possible to inject with different shapes, varying with respect to volume and injection rate. The injection rate however, will have a more or less constant rate during the injection interval. With an injection by hand it is much more difficult to predict the true shape, because the duration and rate can vary a lot. However, for optimal results also a manual injection can be used, as long as the volume and rate is as high as possible.

The Tracer Distribution Model has been shown to be a useful tool to characterize the concentration curve in the feeding arteries, depending on the actual injection shape. The selection of the structure of the TDM was based on a DCE-MRI patient study. The DCE-MRI measurements of the AIF resembled the concentration curves reported in literature [X] [X]. Other TDM structures have been investigated, more and less complex. Also black box models were investigated, varying from 5 to 40 order models, but the results were poor due to the fact that the delay times were hard to estimate. The developed model was a tradeoff between complexity and fitting capability. The TDM model can also be used in other applications based on the distribution of a tracer through the vascular system, e.g. for the use of CT or SPECT. Feng *et al.* also described a model of the arterial time concentration curves with positron emission tomography (PET) [14]. However, this model did not describe relation between the actual shape of the injection and the arterial concentration curve. Therefore the model was insufficient for the usage in this paper.

The fitting of the TDM model and the identification of the pharmacokinetic model was done by means of the standard LSQ method. In the case of the pharmacokinetic model both concentration measurements are subjected to error because they are obtained by a measurement of the DCE-MRI. To not violate the assumptions of the standard LSQ, and because this aspect was not under study, only noise was added to the output, the concentration in the tumor tissue, and the noise on the input, the arterial concentration, has thus been neglected.

The TDM was selected based on the previously described DCE-MRI measurement data. However, these patient studies were conducted with the same injection parameters, i.e. with the same injection rate and volume. For other injection profiles, the arterial curve is a prediction of the TDM and a clinical validation

seems necessary. However, an experimental validation is complicated because various different injection shapes, as also multiple injections, have to be conducted for each patient under the exact same conditions. This results in a difficult clinical setup, because a lot of confusing factors can disturb the DCE-MRI, like the measurement location of both the AIF and the tumor signal [18] and also variation in movement and cardiac output of the patient. Using a simulation study only the factors under study can be analyzed, where the influence of the confusing factors can be reduced. This can not be achieved in a clinical investigation, and for this reason is chosen for a simulation study using synthetic data.

## Conclusion

A theoretic study about the influence of the injection shape on the accuracy of the pharmacokinetic parameters in DCE-MRI was performed. A new Tracer Distribution Model (TDM) was introduced to describe the distribution of the tracer though the vascular system. The model seemed to be applicable for the use of DCE-MRI. A spectral analysis and a "Monte Carlo" simulation study were performed. Both the injection volume as the injection rate has shown a strong influence on the reliability of the calculation of the pharmacokinetic parameters. For optimal experimental conditions, the injection volume and rate should be as high as possible, of course within the clinical range. Small injection rates (below 2mL/s) and small injection volumes (below 15mL) should be avoided, for both a manual injection as the use of an automated pump. Multiple injections decreases the frequency content, because the modulus for the lower frequencies are reduced. This reduction has a large influence on the reliability and a large error can be expected. For this reason a normal single bolus injection is favorable.

**References**


[1] McDonald, D.M. and P.L. Choyke, "Imaging of angiogenesis: form microscope to clinic", *Nature Medicine*, Vol 9, No. 6, pp. 713-725, 2003

[2] Kety, S.S., "The theory and applications of the exchange of inert gas at the lungs and tissues", *Pharmacol Rev*, Vol. 3, pp. 1–41, 1951

[3] Tofts, P.S. and G. Brix, D.L. Buckley, J.L. Evelhoch, E. Henderson, M.V. Knopp, H.B.W. Larsson, T.-Y. Lee, N.A. Mayr, G.J.M. Parker, R.E. Port, J. Taylor, R.M. Weisskoff, "Estimating Kinetic Parameters From Dynamic Contrast-Enhanced T1-Weighted MRI of a Diffusable Tracer: Standardized Quantities and Symbols." *J. Magn. Reson. Imaging*, Vol. 10, pp. 223-232, 1999

[4] Tofts, P.S. "Modeling tracer kinetics in dynamic Gd-DTPA MR imaging", *J. Magn. Reson. Imaging*, Vol. 7, pp. 91–101, 1997

[5] Evelhoch JL,"Key factors in the acquisition of contrast kinetic data for oncology", *J Magn Reson Imaging*, Vol. 10, pp. 254–259, 1999

[6] Tofts, P.S. and A.G. Kermode,"Measurement of the Blood-Brain Barrier Permeability and Leakage Space Using Dynamic MR Imaging - 1. Fundamental Concepts", *Magn. Reson. in Med.*, Vol 17, pp. 357-367, 1991

[7] Buckley, D.L.,"Uncertainty in the Analysis of Tracer Kinetics Using Dynamic Contrast-Enhanced $T_1$-Weighted MRI", *Magn. Reson. in Med.*, Vol. 47, pp. 601-606, 2002

[8] Padhani, A.R., "Dynamic Contrast-Enhanced MRI in Clinical Oncology: Current Status and Future Directions", *J. Magn. Reson. Imaging*, Vol. 16, pp. 407-422, 2002

[9] Taylor, J.S. and P.S. Tofts, R. Port, J.L. Evelhoch, M. Knopp, W.E. Reddick, V.M. Runge, N. Mayr,"MR Imaging of Tumor Microcirculation: Promise for the New Millenium", *J. Magn. Reson. Imaging*, Vol. 10, pp. 903-907, 1999

[10] Henderson, E. and B.K. Rutt, T.Y. Lee,"Temporal Sampling Requirements for the Tracer Kinetics Modeling of Breast Disease", *Magn. Reson. Imaging*, Vol. 16, No. 9, pp. 1057–1073, 1998

[11] Jackson, A. and D.L. Buckley, G.J.M. Parker, "Dynamic Contrast-Enhanced Magnetic Resonance Imaging in Oncology", Springer-Verlag, Berlin, 2005, ISBN: 3-540-42322-2

[12] Girod, B. and R. Rabenstein, A. Stenger, "Signals and Systems", John Wiley & Sons, New York, ISBN: 0-471-98800-6

[13] Ljung, L., "System Identification: Theory for the user", Prentice Hall Inc, New Jersey, 1999. ISBN: 0-13-656695-2

[14] Feng, D. and X. Wang, "Models for Computer Simulation Studies of Input Functions for Tracer Kinetic Modeling with Positron Emission Tomography", *Int. J. Biome. Compu.*, Vol 32, pp. 95-110, 1993

[15] Madsen, M.T., "A Simplified Formulation of the Gamma-Variate Function", *Phys. Med. Biol.*, Vol. 32, No. 7, pp. 1597-1600, 1992

[16] Davenport, R., "The Derivation of the Gamma-Variate Relationship for Tracer Dilution Curves", *J. Nucl. Med.*, Vol. 24, No. 10, pp. 945-948, 1983

[17] Music, R.F. and A.D. Nelson, G.M. Saibel, F. Miraldi, "Optimal Experiment Design for PET Quantification of Receptor Concentration", *IEEE Trans. Med. Imaging*, Vol 15, No 1, pp. 1-12, 1996

[18] Ruediger E. Port and M.V. Knopp,G. Brix, "Dynamic Contrast-Enhanced MRI Using Gd-DTPA: Interindividual Variability of the Arterial Input Function and Consequences for the Assessment of Kinetics in Tumors", *Magn. Reson. Med.*, Vol. 45, pp. 1030–1038, 2001

[19] Yang C. and G.S. Karczmar, M. Medved, W.M. Stadler, "Estimating the Arterial Input Function Using Two Reference Tissues in Dynamic Contrast-Enhanced MRI Studies: Fundamental Concepts and Simulations", Magn. Reson. Med., Vol. 52, pp. 1110–1117, 2004

[20] Lussanet, Q.G. and W.H. Backes, A.W. Griffioen, A.R. Padhani, C.I. Baeten, A. Baardwijk, P. Lambin, G.L. Beets, J.M.A. Engelshoven, R.G.H. Beets-Tan, "Dynamic Contrast-Enhanced Magnetic Resonance Imaging of Radiation Therapy Induced Microcirculation Changes in Rectal Cancer", *In press: Int. J. Radiation Oncology Biol. Phys., Vol. xx, No. x, pp. xxx, 2005*

[21] Lopata, R. and W. Backes, P.P.J. van den Bosch, N.A.W. van Riel,
"On the Identifiability of Pharmacokinetic Parameters in Dynamic Contrast-Enhanced Imaging"

[22] Port, R.E. and M.V. Knopp ....
"Multicompartment analysis of gadolinium chelate kinetics: blood-tissue exchange in mammary tumors as monitored by dynamic MR imaging"
J. Magn. Reson. Imag. ,Vol. 10 (1996), p. 233-241

[23] Fritz-Hansen, T. and T. Rostrup...
"Measurement of the arterial concentration of Gd-DTPA using MRI: a step toward quantitative perfusion imaging"
Magn. Reson. Med, Vol. 36 (1996), p.225-231

## Appendix

*A. The Rectangular Shape*

When we assume, for the convenience, that the injection shape resembles a block, in stead of a trapezium shape, from equation 3 follows:

$$E_f = \int_{-\infty}^{\infty} IR^2 dt = \int_0^{\tau} IR^2 dt = IR^2 \cdot \tau = IR \cdot IV \tag{13}$$

with τ as the injection duration and IR as the injection rate. It is apparent that the injection with the highest rate and highest volume will have the highest frequency content. To see how the energy (the frequency content) is divided over the spectrum, the spectrum of the rectangular injection pulse can be calculated with:

$$F(w) = \frac{IR\tau}{w}\sin\left(\frac{w\tau}{2}\right) = IR\tau \cdot \mathrm{sinc}\left(\frac{w\tau}{2\pi}\right) = IV \cdot \mathrm{sinc}\left(\frac{w\tau}{2\pi}\right) \tag{14}$$

where IR is the injection rate (mL/s) and τ the injection duration (sec). The arterial concentration will be a 'smoothed' version of the injection shape, because of the low-pass filtering of the TDM.

In the figure 10 several rectangle shapes are displayed, and the corresponding frequency spectrum.

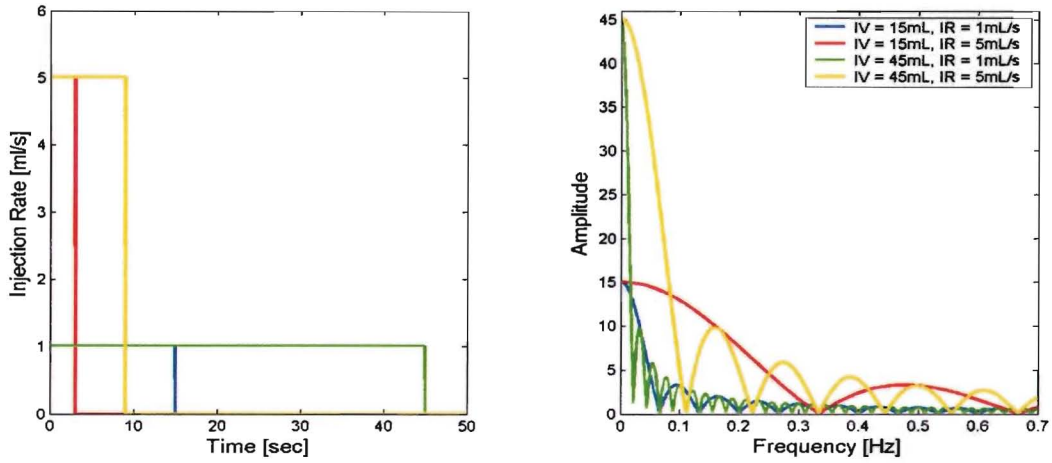


*Figure 10: Rectangular Shape in the time (left) and frequency (right) domain.*

The steady state gain (gain at $f = 0$Hz) is equal to the injection volume, and every spike is zero at $\frac{n}{\tau}$ [Hz], with n=1,2,…., and τ the injection duration (sec). Form both figure 6c and 10 can be observed, that there exits no tradeoff that one injection shape has the optimal frequency content for the lower spectrum and another shape the optimum for the higher frequencies. The highest volume and the highest injection rate always has the optimum frequency content for both the lower as the higher frequencies.

For the trapezium shape, this equation 13 is altered to:

$$E_f = IR \cdot IV - \frac{1}{3} IR^2 \alpha = IR^2(\tau - \frac{1}{3}\alpha) \tag{15}$$

where α is the duration of the rising and falling slope (sec). For each extra injection (with multiple injections) an extra rising and falling slope is added, and energy equivalently to $\frac{1}{3} IR^2 \alpha$ is lost. To display the difference of the rectangular shape with the trapezium shape, figure 11 shows the differences.

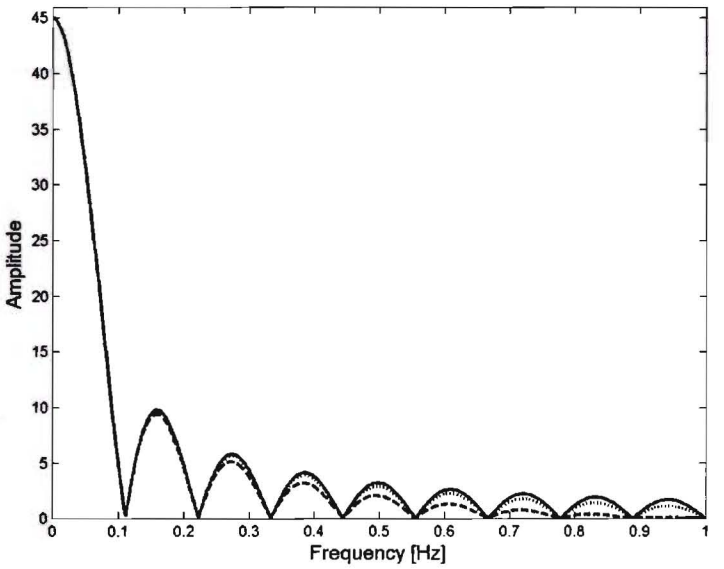


*Figure 11: The frequency spectrum of the rectangular shape (solid) and the trapezium shape with a rising and falling slope of 1 sec (dashed). Also the spectrum of a trapezium shape is shown with a rising and falling slope of 0.5 sec (dotted). Injection Volume is 45mL and Injection Rate 5mL.*

The slopes decrease the higher frequencies, as can be seen from figure 11. The rectangular spectrum (solid) is the most ideal, because no energy is lost in the slopes which yield the best excitation for the higher frequencies. This is worst for the trapezium shape where a decrease of the higher frequencies can be seen. Even no frequencies above 1Hz appear in the signal, when the slopes duration is 1 sec . When the rising and falling slope duration is set to 0.5 sec, the decrease is much less, and a better excitation is the result.